Design Rule for Colloidal Crystals of DNA-Functionalized Particles

Francisco J. Martinez-Veracoechea,[1] Bianca M. Mladek,[1,2] Alexei V. Tkachenko,[3] and Daan Frenkel[1]

[1]*Department of Chemistry, University of Cambridge, Lensfield Road, Cambridge, CB2 1EW, United Kingdom*

[2]*Department of Structural and Computational Biology, Max F. Perutz Laboratories GmbH, Campus Vienna Biocenter 5, Vienna 1030, Austria*

[3]*Center for Functional Nanomaterials, Brookhaven National Laboratory, Upton, New York 11973-5000, USA.*

(Received 6 April 2011; published 20 July 2011; corrected 22 July 2011)

We report a Monte Carlo simulation study of the phase behavior of colloids coated with long, flexible DNA chains. We find that an important change occurs in the phase diagram when the number of DNAs per colloid is decreased below a critical value. In this case, the triple point disappears and the condensed phase that coexists with the vapor is always liquid. Our simulations thus explain why, in the dilute solutions typically used in experiments, colloids coated with a small number of DNA strands cannot crystallize. We understand this behavior in terms of the discrete nature of DNA binding.

DOI: 10.1103/PhysRevLett.107.045902 PACS numbers: 65.20.Jk, 64.70.dg, 65.40.−b, 81.16.Dn

The specificity of binding between complementary DNA strands opens the way to the rational design of complex, nanostructured materials [1–4]. For example, a colloid can be functionalized with DNA chains terminated by a short single-stranded DNA (ssDNA) sequence [5]. These ''sticky'' ssDNA ends can be designed to bind specifically and reversibly to complementary sticky ends grafted to other colloids. In this way, it is in principle possible to program the self-assembly of complex structures into the DNA coating of the constituent building blocks [6]. However, progress in the assembly of truly complex supra-molecular assemblies has been thus far limited by an incomplete understanding of the underlying principles that determine the phase behavior and kinetics of such systems [6]. In particular, entropic effects, somewhat underappreciated, have been shown to be both complex and counterintuitive [7–10].

DNA-driven crystallization is arguably the area where most progress has been made [3,11–13]. Pure, single-component systems of gold nanoparticles coated with short, self-complementary DNA strands have been observed to crystallize into a face-centered-cubic (fcc) structure [2,14]. Alternatively, binary mixtures of gold nanoparticles have been shown to assemble into a body-centered-cubic (bcc) structure [11,14,15].

In an effort to better understand the factors that control the crystallization of DNA-coated systems, computer simulations prove to be a valuable tool [16–18]. In earlier work [9,10] we showed using simulations that, similar to systems of patchy colloids [19], binary mixtures of colloids coated with long DNA can exhibit a transition from a dilute to a concentrated amorphous suspension. This ''vapor-liquid'' equilibrium can only be obtained if the hybridization free energy per bond (βf_{hyb}) exceeds a critical strength. Since $\beta = 1/kT$, where k is Boltzmann's constant and T the absolute temperature, such strong binding can often be achieved by cooling the system or by modification of the sequence and length of the sticky ends. In the simulations of Ref. [11] that focused on colloids functionalized with at most seven DNA chains (i.e., a ''valence'' $\kappa \leq 7$), spontaneous crystallization was not observed. Yet, at high volume fractions, a stable crystalline phase must form because hard-sphere colloids freeze at high pressures due to purely entropic reasons [20,21]. However, high-pressure crystals cannot coexist with the dilute colloidal solutions that are typically used in experiments on DNA-coated colloids [2,3,11,14,15,22].

In the present Letter we investigate under what conditions one should observe crystallization of a binary mixture of colloids (labeled A and B) coated with long DNA directly from dilute solutions. To study DNA-induced freezing we use a coarse-grained model where colloids are represented as hard spheres with a radius $R_c = 3R_g$, where R_g is the radius of gyration of the DNA strands. As we are interested in the generic features of the phase diagram, we use a model of the DNA-coated colloids where each DNA chain is described as a single soft ''blob''; i.e., DNA chains interact with each other through an effective, Gaussian potential [23]. This is an oversimplification—but it is adequate for micron-sized colloids coated with long, double-stranded DNA or for nanoparticles with ssDNA chains. DNA coils are anchored to the surface of the colloid with an isotropic harmonic spring that allows them to freely move on the surface of the colloid. We summarize the relevant details of this model in the Supplemental Material [24] . For further details, we refer the reader to Ref. [9].

Bonding between complementary sticky ends is treated in an ''on-off'' manner. Type-A DNA can only bind to type-B and each DNA chain can only bind to a single complementary chain at a time. Thus, when two DNA chains are hybridized they become connected by an additional harmonic spring (see Refs. [9,10]) that is removed when the bond is broken. The formation and breaking of

bonds is carried out in special Monte Carlo moves [9] described in [24].

In the present study we use a combination of non-Boltzmann sampling [25–27] and constant-pressure Monte Carlo simulations to determine phase coexistence as described in detail in Ref. [9]. Non-Boltzmann sampling schemes have the advantage that they provide the system's free energy (up to an additive constant) as a function of the relevant thermodynamic variables [25,28–30], in this case the volume fraction of bare colloids (η) and the hybridization free energy per bond (βf_{hyb}).

We simulated a mixture of A- and B-type DNA-coated colloids where each colloid is coated with $\kappa = 16$ DNA chains. The Helmholtz free energy (βA) was obtained as a function of η for different values of βf_{hyb} as shown in Fig. 1(a). Two minima are observed, corresponding to a liquidlike phase and a CsCl crystal phase. The crystal structure was identified by examination of the snapshots and through the radial distribution function [see Fig. 1(b)]. In the CsCl structure, two simple cubic lattices interpenetrate, with each colloid surrounded by eight opposite-type neighbors. As the A and B type colloids are identical (except for the sticky end of their DNA), this structure is often referred to simply as bcc in the DNA-coated colloid literature [11,14,15]. We will use the latter convention (i.e., bcc) in the remainder of this work.

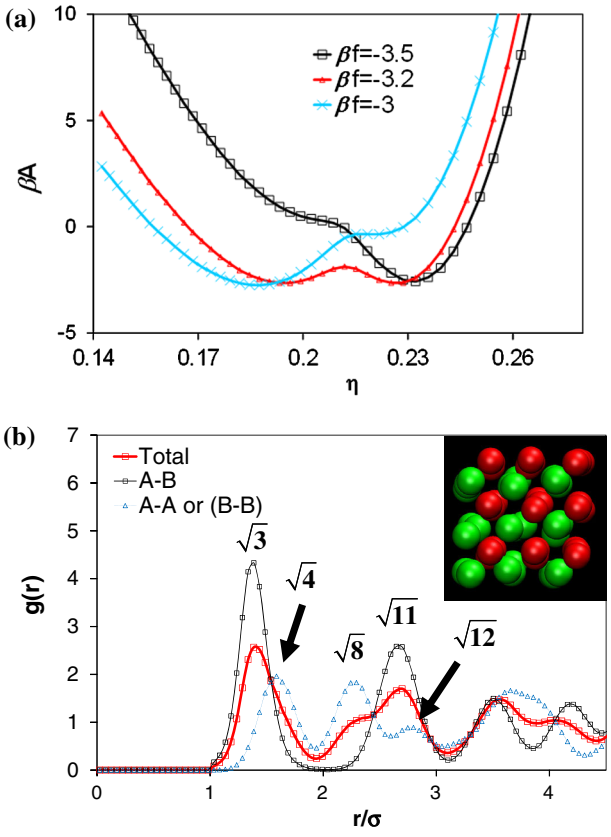

FIG. 1 (color online). Simulations of colloids coated with $\kappa = 16$ DNA chains. (a) The total Helmholtz free energy (βA) as a function of η for different binding strengths (βf_{hyb}). The two minima correspond to the liquid (left) and CsCl crystal (right) phases. (b) Pair distribution function $g(r)$ and snapshot of the simulated crystal phase. We show the total $g(r)$, the "opposite-type" A-B $g(r)$, and the "same-type" A-A (or B-B) $g(r)$. The peaks are located in the positions consistent with the bcc structure.

The only crystal phase that formed spontaneously during the simulations in the concentration range that we studied was the bcc phase. Moreover, calculation of the free energy of distinct candidate crystal structures by thermodynamic integration [31–33] showed that the bcc phase always has a lower free energy than the other candidate phases (see [24]). This finding gives us confidence that the bcc phase is robustly preferred over other crystal structures over the range of volume fractions studied.

An important quantity that determines the mechanical stability of colloidal crystals is the number of DNA-mediated links between neighboring colloids. In Fig. 2 we show the average number of colloids (τ) connected to a given colloid through one or more DNA links as a function of η, for different values of κ, and in the limit of low-temperature or strong hybridization (i.e., $\beta f_{\mathrm{hyb}} \to -\infty$). We find that the regions of the phase diagram where $\tau > 6$ correlate with the appearance of stable bcc crystals. For each value of κ shown in Fig. 2, τ varies relatively slowly at high and low η, corresponding with the crystal and liquid phases, respectively. However, in the range of η where $\tau \sim 6$, we observe a rapid variation of the value of τ, consistent with the melting of the crystal structure.

The finding that the crystal structures are only stable when $\tau \geq 6$ is consistent with an isostaticity argument: a necessary condition for the mechanical stability of a 3D system of smooth, spherical particles is that each particle is on average bonded to at least 6 different neighbors (see [24]). For the crystals considered here, mechanical stability is due to the intercolloidal DNA-DNA bonds rather than to the colloid-colloid hard-core repulsion. This observation is supported by the fact that the first peak of the radial

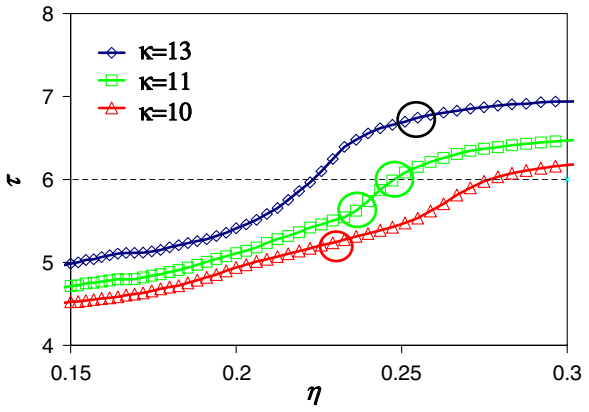

FIG. 2 (color online). The average number of colloids (τ) to which each colloid is directly connected as a function of η, for different values of κ and in the limit of strong hybridization. The location of the minimum in free energy is indicated with a circle for each value of κ.

distribution function $g(r)$ [Fig. 1(b)] is located at around 1.4 times the colloidal diameter ($\sigma = 2R_c$) and not at contact (i.e., $r/\sigma = 1$).

Crystallization experiments on DNA-coated colloids usually start with dilute solutions; thus, the crystal phase will be observed only when it can coexist directly with the colloidal "vapor" phase. In principle, to locate the crystal-vapor coexistence curve we need to know the vapor pressure, P_{vap}, as a function of βf_{hyb}. In practice, we need not compute the vapor pressure as it is very small for the colloidal valences studied in this work (i.e., $9 \leq \kappa \leq 16$), and we can to a good approximation assume that P_{vap} is zero. Indeed, already for systems with $\kappa = 7$ the vapor pressure is negligible almost up to the critical point (e.g., for $\kappa = 7$, $P_{\text{vap}} \sim 10^{-7} kT/R_g^3$). When $P_{\text{vap}} \approx 0$, the vapor phase will coexist only with the phase (liquid or crystal) that has the lowest value of the Helmholtz free energy. We therefore used free energy calculations to estimate the low-temperature equilibrium phase diagram of DNA-coated colloids for different valences κ (Fig. 3). Note that the phase behavior at $\beta f_{\text{hyb}} = -20$ is essentially the same as in the strong hybridization limit (i.e., $\beta f_{\text{hyb}} \to -\infty$), and therefore we do not extend our diagrams beyond this value. Surprisingly, we observe that there exists a crossover in behavior: when $\kappa < 11$ the liquid phase is always more stable (at zero pressure) than the crystal phase, even in the limit of zero temperature (i.e., $\beta f_{\text{hyb}} \to -\infty$). Hence, systems with $\kappa < 11$ have no triple point and condensation at low temperatures is into the liquid rather than the crystal phase: a striking feature that resembles the phase behavior of helium. For $\kappa > 11$, we obtain direct vapor-crystal coexistence and therefore a vapor-liquid-crystal triple point appears. Yet, at very low temperatures crystallization may be kinetically prevented by the appearance of a gel phase.

The finding that for small numbers of grafted DNA, coexistence between a dilute solution and the crystal phase is not possible, offers an explanation for the observation of Xiong *et al.* [15] that crystallization of DNA-coated gold nanoparticles requires a minimum number of "DNA-linkers" between 8 and 12. When $\kappa = 11$, two minima of roughly similar free energy are observed in the limit of strong hybridization. Since the liquid phase minimum is slightly lower, the phase diagram shown in Fig. 3(b) does not have a triple point, and crystallization directly from the vapor cannot occur anymore. However, the *precise* value of κ at which the triple point disappears is likely to be slightly model dependent.

That the valence κ controls whether there exists direct vapor-crystal equilibrium is a consequence of the fact that as κ is decreased it becomes entropically less favorable to form bonds with more than six neighbors at a time. In the bcc phase each colloid is surrounded by eight opposite-type neighbors with which bonds can be made—yet a particle need not be bonded to all its neighbors simultaneously. If we assume that the probability of forming a DNA link with each neighbor is equal and independent of the number of bonds already formed, then the average number of connected neighbors (τ) can be estimated from a multinomial distribution. For this purely entropic model, the average value of τ decreases as κ is decreased (e.g., $\tau = 6.39$ for $\kappa = 12$,

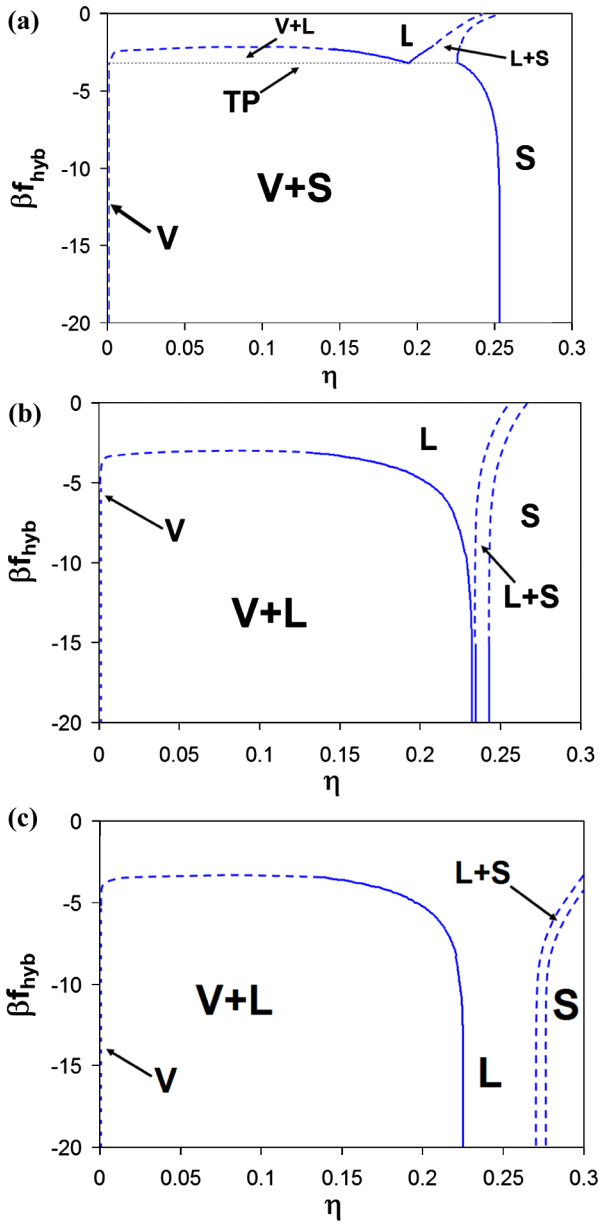

FIG. 3 (color online). Phase diagram of the DNA-coated colloids in the plane βf_{hyb} vs η for different values of κ. Dashed lines only represent a qualitative description of the expected phase behavior. Since a single fluid phase is observed for the weak-binding regime (i.e., $0 < \beta f_{\text{hyb}} < +\infty$) we limit our plots to $\beta f_{\text{hyb}} = 0$. Also, other phases may be stable for $\eta > 0.30$ but they will not coexist directly with the vapor phase. (a) $\kappa = 16$, the system displays a triple point (TP) where the vapor phase (V), the liquid phase (L), and the bcc solid phase (S) coexist. (b) $\kappa = 11$, the system no longer presents a TP. The vapor-liquid coexistence envelope ($V + L$) and the liquid-crystal envelope ($L + S$) are always separated by a narrow region where the pure L phase is stable. (c) $\kappa = 10$, the $L + S$ envelope shifts to increasing values of η.

$\tau = 5.90$ for $\kappa = 10$, and $\tau = 5.25$ for $\kappa = 8$). Thus, below a critical value of the valence ($\kappa \sim 11$ in this work) it becomes more favorable to melt the crystal than to pay the entropic penalty required to retain six connected neighbors. This unusual phase behavior is a direct consequence of the discrete nature of DNA binding: each chain can only form one bond at the time. Therefore, the phase behavior of this system cannot be captured by an effective isotropic pair-potential between colloids, where a particle interacts simultaneously with all its neighbors. Thus, the many-body nature of the colloid-colloid interactions becomes crucially important for the relatively low DNA coverage (i.e., $\kappa \leq 16$) employed in this work.

In conclusion, we employed computer simulations to study the crystallization of a simple model for colloids coated with flexible DNA of a size comparable to the colloid's radius (i.e., $R_g = R_c/3$). We found that colloids functionalized with less than 11 DNA chains present a phase diagram where no vapor-liquid-crystal triple point exists. Thus, direct coexistence between a dilute vapor phase and a crystalline phase can only occur when each colloid is coated with more than 11 DNA chains. The crystalline phase was always observed to have bcc (CsCl) symmetry. We found that particles in the crystals are on average connected to at least six of the neighbors in agreement with the requirement of mechanical stability. Finally, we observed that the complex behavior displayed by colloids coated with a few, long DNA chains crucially depends on the discrete nature of bonding and on how these bonds can be rearranged among the neighbors. In the current study we have considered a model where the anchoring points of the DNA chains can move freely on the surface of the colloids. We expect that crystallization can be facilitated if we fix the anchoring points of the DNA chains at locations consistent with the symmetry of the desired crystal [16,17,34]. Such precise control, however, has hitherto proven difficult to obtain [35].

F. J. M. V. thanks the ERC for support (Advanced Grant agreement 227758). B. M. M. acknowledges EU funding via FP7-PEOPLE-IEF-2008 No. 236663 and the MFPL VIPS program. D. F. acknowledges support from a Wolfson Merit Award (Royal Society of London). Research partially carried out at the CFN, BNL, which is supported by the US DOE, Office of BES, under Contract No. DE-AC02-98CH10886.

[1] C. A. Mirkin, R. L. Letsinger, R. C. Mucic, and J. J. Storhoff, Nature (London) **382**, 607 (1996).
[2] R. J. Macfarlane, B. Lee, H. D. Hill, A. J. Senesi, S. Seifert, and C. A. Mirkin, Proc. Natl. Acad. Sci. U.S.A. **106**, 10 493 (2009).
[3] D. Nykypanchuk, M. M. Maye, D. van der Lelie, and O. Gang, Nature (London) **451**, 549 (2008).
[4] A. Stadler, C. Chi, D. van der Lelie, and O. Gang, Nanomedicine **5**, 319 (2010).
[5] M. E. Leunissen, R. Dreyfus, F. C. Cheong, D. G. Grier, R. Sha, N. C. Seeman, and P. M. Chaikin, Nature Mater. **8**, 590 (2009).
[6] M. E. Leunissen, R. Dreyfus, R. J. Sha, T. Wang, N. C. Seeman, D. J. Pine, and P. M. Chaikin, Soft Matter **5**, 2422 (2009).
[7] R. Dreyfus, M. E. Leunissen, R. J. Sha, A. V. Tkachenko, N. C. Seeman, D. J. Pine, and P. M. Chaikin, Phys. Rev. Lett. **102**, 048301 (2009).
[8] M. E. Leunissen, R. Dreyfus, R. Sha, N. C. Seeman, and P. M. Chaikin, J. Am. Chem. Soc. **132**, 1903 (2010).
[9] F. J. Martinez-Veracoechea, B. Bozorgui, and D. Frenkel, Soft Matter **6**, 6136 (2010).
[10] B. Bozorgui and D. Frenkel, Phys. Rev. Lett. **101**, 045701 (2008).
[11] H. M. Xiong, D. van der Lelie, and O. Gang, J. Am. Chem. Soc. **130**, 2442 (2008).
[12] A. V. Tkachenko, Phys. Rev. Lett. **89**, 148303 (2002).
[13] A. J. Kim, P. L. Biancaniello, and J. C. Crocker, Langmuir **22**, 1991 (2006).
[14] S. Y. Park, A. K. R. Lytton-Jean, B. Lee, S. Weigand, G. C. Schatz, and C. A. Mirkin, Nature (London) **451**, 553 (2008).
[15] H. M. Xiong, D. van der Lelie, and O. Gang, Phys. Rev. Lett. **102**, 015504 (2009).
[16] W. Dai, S. K. Kumar, and F. W. Starr, Soft Matter **6**, 6130 (2010).
[17] F. Vargas Lara and F. W. Starr, Soft Matter **7**, 2085 (2011).
[18] R. T. Scarlett, M. T. Ung, J. C. Crocker, and T. Sinno, Soft Matter **7**, 1912 (2011).
[19] E. Bianchi, J. Largo, P. Tartaglia, E. Zaccarelli, and F. Sciortino, Phys. Rev. Lett. **97**, 168301 (2006).
[20] B. J. Alder and T. E. Wainwright, J. Chem. Phys. **27**, 1208 (1957).
[21] W. W. Wood and J. D. Jacobson, J. Chem. Phys. **27**, 1207 (1957).
[22] N. Geerts, T. Schmatko, and E. Eiser, Langmuir **24**, 5118 (2008).
[23] C. Pierleoni, B. Capone, and J. P. Hansen, J. Chem. Phys. **127**, 171102 (2007).
[24] See Supplemental Material at http://link.aps.org/supplemental/10.1103/PhysRevLett.107.045902 for details about the model and methods.
[25] C. R. A. Abreu and F. A. Escobedo, J. Chem. Phys. **124**, 054116 (2006).
[26] B. A. Berg and T. Neuhaus, Phys. Rev. Lett. **68**, 9 (1992).
[27] F. J. Martinez-Veracoechea and F. A. Escobedo, J. Phys. Chem. B **112**, 8120 (2008).
[28] F. J. Martinez-Veracoechea and F. A. Escobedo, J. Chem. Phys. **125**, 104907 (2006).
[29] F. J. Martinez-Veracoechea and F. A. Escobedo, Macromolecules **42**, 1775 (2009).
[30] J. R. Errington, J. Chem. Phys. **118**, 9915 (2003).
[31] D. Frenkel and B. Smit, *Understanding Molecular Simulation* (Academic Press, San Diego, CA, 2002).
[32] B. M. Mladek, P. Charbonneau, and D. Frenkel, Phys. Rev. Lett. **99**, 235702 (2007).
[33] B. M. Mladek, P. Charbonneau, C. N. Likos, D. Frenkel, and G. Kahl, J. Phys. Condens. Matter **20**, 494245 (2008).
[34] E. G. Noya, C. Vega, J. P. K. Doye, and A. A. Louis, J. Chem. Phys. **132**, 234511 (2010).
[35] K. Suzuki, K. Hosokawa, and M. Maeda, J. Am. Chem. Soc. **131**, 7518 (2009).